EBioMedicine 27 (2018) 304–316

Contents lists available at ScienceDirect

EBioMedicine

journal homepage: www.ebiomedicine.com

Research Paper

Zinc Deficiency via a Splice Switch in Zinc Importer ZIP2/SLC39A2 Causes Cystic Fibrosis-Associated MUC5AC Hypersecretion in Airway Epithelial Cells☆

Shunsuke Kamei [a,b], Haruka Fujikawa [a,b], Hirofumi Nohara [a,b], Keiko Ueno-Shuto [c], Kasumi Maruta [a], Ryunosuke Nakashima [a], Taisei Kawakami [a], Chizuru Matsumoto [a], Yuki Sakaguchi [a], Tomomi Ono [a], Mary Ann Suico [a], Richard C. Boucher [d], Dieter C. Gruenert [e], Toru Takeo [f], Naomi Nakagata [f], Jian-Dong Li [g], Hirofumi Kai [a,*], Tsuyoshi Shuto [a,**,1]

[a] Department of Molecular Medicine, Graduate School of Pharmaceutical Sciences, Kumamoto University, 5-1 Oe-Honmachi, Chuo-ku, Kumamoto 862-0973, Japan
[b] Program for Leading Graduate Schools "HIGO (Health life science: Interdisciplinary and Glocal Oriented) Program", Kumamoto University, 5-1 Oe-Honmachi, Chuo-ku, Kumamoto 862-0973, Japan
[c] Laboratory of Pharmacology, Division of Life Science, Faculty of Pharmaceutical Sciences, Sojo University, 4-22-1 Ikeda, Nishi-ku, Kumamoto 860-0082, Japan
[d] Marsico Lung Institute, University of North Carolina at Chapel Hill, Chapel Hill, NC, USA
[e] Head and Neck Stem Cell Lab, University of California, San Francisco, 2340 Sutter St, Box 1330, N331, San Francisco, CA 94115, USA
[f] Division of Reproductive Engineering, Center for Animal Resources and Development (CARD), Kumamoto University, 2-2-1 Honjo, Chuo-ku, Kumamoto 860–0811, Japan
[g] Center for Inflammation, Immunity & Infection, Institute for Biomedical Sciences, Georgia State University, 714 Petit Science Center, 100 Piedmont Ave SE, Atlanta GA30303, USA

ARTICLE INFO

Article history:
Received 3 September 2017
Received in revised form 15 December 2017
Accepted 19 December 2017
Available online 20 December 2017

Keywords:
ZIP2
CFTR
ENaC
Splicing isoform
Mucus hypersecretion
Cystic fibrosis

ABSTRACT

Airway mucus hyperproduction and fluid imbalance are important hallmarks of cystic fibrosis (CF), the most common life-shortening genetic disorder in Caucasians. Dysregulated expression and/or function of airway ion transporters, including cystic fibrosis transmembrane conductance regulator (CFTR) and epithelial sodium channel (ENaC), have been implicated as causes of CF-associated mucus hypersecretory phenotype. However, the contributory roles of other substances and transporters in the regulation of CF airway pathogenesis remain unelucidated. Here, we identified a novel connection between CFTR/ENaC expression and the intracellular Zn^{2+} concentration in the regulation of MUC5AC, a major secreted mucin that is highly expressed in CF airway. CFTR-defective and ENaC-hyperactive airway epithelial cells specifically and highly expressed a unique, alternative splice isoform of the zinc importer ZIP2/SLC39A2 (ΔC-ZIP2), which lacks the C-terminal domain. Importantly, ΔC-ZIP2 levels correlated inversely with wild-type ZIP2 and intracellular Zn^{2+} levels. Moreover, the splice switch to ΔC-ZIP2 as well as decreased expression of other ZIPs caused zinc deficiency, which is sufficient for induction of MUC5AC; while ΔC-ZIP2 expression *per se* induced ENaC expression and function. Thus, our findings demonstrate that the novel splicing switch contributes to CF lung pathology *via* the novel interplay of CFTR, ENaC, and ZIP2 transporters.

1. Introduction

Airway homeostasis of fluid volume, viscosity, and chemical components is essential for maintaining mucus clearance and keeping the lungs free from microbial infections, which is mainly regulated by epithelial ion transporters. One well-known and characterized transporter is the cystic fibrosis transmembrane conductance regulator (CFTR), a cyclic AMP-dependent Cl^- channel that controls fluid and ion transport across the lung epithelium. Consistently, CFTR dysfunction causes an imbalance between fluid absorption and secretion, which leads to the development of cystic fibrosis (CF), a genetic disease characterized by hyperviscoelastic mucus secretions in the lungs (Haq et al., 2016; Elborn, 2016). The epithelial sodium channel (ENaC) is also a major

☆ Tribute: We would like to dedicate this paper and thus acknowledge the outstanding contribution by Dr. Dieter C. Gruenert to the field of airway epithelial biology. He will be sadly missed by his colleagues and friends. Dr. Dieter C. Gruenert passed away on April 10, 2016.

* Corresponding author.
** Corresponding author at: Department of Molecular Medicine, Graduate School of Pharmaceutical Sciences, Kumamoto University, 5-1 Oe-Honmachi, Chuo-ku, Kumamoto 862-0973, Japan.
E-mail addresses: hirokai@gpo.kumamoto-u.ac.jp (H. Kai), tshuto@gpo.kumamoto-u.ac.jp (T. Shuto).
[1] Lead Contact.

https://doi.org/10.1016/j.ebiom.2017.12.025

ion transporter that is expressed in the apical membrane of airway epithelial cells in the lungs. ENaC activation helps the generation of a concentration gradient of sodium ions, followed by water absorption by cells; however, its hyperactivation can result in airway mucus hyperproduction and dysregulated airway clearance (Almaça et al., 2013; Astrand et al., 2015; Haq et al., 2016). Indeed, the expression and function of ENaC were inversely associated with lung function in CF patients (Boucher, 2007). Moreover, we and others have reported that mice with airway-specific overexpression of βENaC (βENaC-transgenic [Tg] mice) exhibit the critical pulmonary phenotypes of CF, such as mucus obstructive, airway inflammatory, and emphysematous phenotypes (Mall et al., 2004; Johannesson et al., 2012; Shuto et al., 2016). These findings imply that CFTR and ENaC are essential ion transporters that control airway fluid homeostasis. Importantly, because an inverse relationship between CFTR and ENaC functions has been widely accepted in CF research fields (Mall and Galietta, 2015), hyperactive-ENaC condition is increasingly being recognized as a CF-like condition. Notably, despite the contribution of Cl^- and Na^+ imbalance in CF airway, little is known about the role of other substances and their transporters in the regulation of CF-associated airway phenotypes.

The zinc ion (Zn^{2+}) plays an essential role in many biological activities in different organisms by regulating the proper functions of zinc-finger proteins, which mainly control cellular transcription, and zinc-containing enzymes involved in the antioxidant defense system (Vallee and Falchuk, 1993; Andreini et al., 2006; Hara et al., 2017). Thus, zinc deficiency causes a variety of symptoms associated with oxidative stress, inflammation, aging, and other symptoms (Prasad, 2013; Fukada et al., 2011). One interesting research topic is how the zinc ion functions in transducing cellular signals (referred to as "zinc signaling"), like the calcium ion (Ca^{2+}) (Liang et al., 2016; Fukada et al., 2011). The importance of the zinc ion and its related signal pathways has been described for numerous aspects of, not only physiology, but also in the pathology of diseases, such as diabetes, Alzheimer's disease, and cancer (Miao et al., 2013; Duce et al., 2010; Grattan and Freake, 2012). Moreover, based on the facts that zinc levels are dysregulated (lower in blood and higher in sputum) in CF patients (Gray et al., 2010; Van Biervliet et al., 2007; Damphousse et al., 2014) and that zinc supplementation can improve CF phenotypes (respiratory function and the incidence of infection) (Van Biervliet et al., 2008; Abdulhamid et al., 2008), zinc dysregulation may also be a possible pathophysiological hallmark of CF. However, these findings could only explain the importance of zinc in airway in a nutritional but not as cellular and molecular aspects. Thus, how zinc levels are controlled under pathological CF conditions and exactly which molecules are responsible for zinc regulation in CF airway epithelial cells are interesting questions to be investigated.

In this study, we first showed decreased levels of intracellular zinc as a common feature in both CFTR-defective CF airway epithelial and ENaC-hyperactive, CF-like airway epithelial cells. We also determined the down-regulation of several zinc importer ZIPs (Zrt-, Irt-like proteins) in CF and CF-like airway cells. Importantly, electrophoretic analysis revealed that a novel and unexpected, pathologically relevant splicing switch in zinc importer ZIP2 (Zrt-, Irt-like protein 2)/SLC39A2 is dominantly involved in intracellular zinc depletion in CF and CF-like airway epithelial cells. This study shows that zinc deficiency via the unique splicing switch of ZIP2 is crucial for CF lung pathology, especially with respect to the induction of MUC5AC, a major secreted mucin that is highly expressed in CF airway, which is exerted by the novel interplay of CFTR, ENaC, and ZIP2 transporters.

2. Materials and Methods

2.1. Cell Culture

The human bronchial 16HBE14o- (Cozens et al., 1992), CFBE41o- (Cozens et al., 1994), βγENaC-stable 16HBE14o- (Caldwell et al., 2005), and WT or ΔF508 CFTR-stable CFBE41o- (Illek et al., 2008) cell lines were previously generated and grown in fibronectin/bovine serum albumin (BSA)-coated dishes from Invitrogen (Mizunoe et al., 2012). The CFBE41o- cell line was reported to be homozygous for the ΔF508 CFTR mutation (ΔF508/ΔF508) and retain many phenotypes of CF bronchial epithelial cells (Mizunoe et al., 2012). These cells were maintained in minimum essential medium. 293 T cells were maintained in Dulbecco's modified Eagle's medium and used for lentivirus transduction. These media were supplemented with 10% fetal bovine serum, 100 U/mL of penicillin, and 100 mg/mL of streptomycin. Primary normal (NHBE) and primary DHBE-CF cells were purchased from Takara and maintained as described previously (Mizunoe et al., 2012). All cells were cultured in a humidified incubator at 37 °C with 5% CO_2.

To induce intracellular zinc depletion, 16HBE14o- cells were treated with TPEN (Dojindo) or dimethyl sulfoxide (DMSO) alone for 2 or 6 h. Concurrent treatment with 20 μM $ZnCl_2$ (Wako) was performed to abrogate the zinc-depletion effect.

2.2. siRNA Transfections and Lentivirus Infections

For gene-knockdown experiments, ZIP2, ZIP4, ZIP8, ZIP10, and ZIP14 siRNA SMARTpools (GE Dharmacon) and control GL2 siRNA (Suico et al., 2014) were transfected using RNAiMAX (Thermo Fisher Scientific), following the manufacturer's recommended protocol.

For lentivirus production, the full-length human ΔC-ZIP2 cDNA sequence was generated and inserted into the *Eco*RI site of the pLVSIN-IRES-ZsGreen1 vector (Takara). The EF1α promoter and puromycin-resistance gene were additionally inserted into the 5′-*Not*I and 3′-*Bam*HI sites for drug selection. The splice site-mutated (IVS1 + T > C) and stop codon-inserted (K8X) ΔC-ZIP2 mutants were generated utilizing the QuikChange II Site-Directed Mutagenesis Kit (Agilent). 293 T cells were transfected with the pLVSIN, pMD2.G, and pCMVR8.74 vectors for 3 days. The supernatant was collected and incubated with Lenti-X Concentrator (Takara) for virus concentration. Virus-infected 16HBE14o- stable transductants overexpressing the genes of interest were established by selection in 4 μg/mL puromycin selection.

2.3. RNA Isolation, cDNA Synthesis, and PCR Analysis

Total RNA was isolated from cells and mouse lung tissues using the RNAiso Plus Kit (Takara) and cDNA synthesis was performed using the PrimeScript RT Regent Kit (Takara). Real-time quantitative RT-PCR analysis was performed as described previously (Shuto et al., 2016). α-, β-, and γ-ENaC-expression plasmids (pCMV-Tag5A) were produced previously (Sugahara et al., 2009) and used to measure the total amounts of mRNA. The sequences of primers used for real-time quantitative RT-PCR are shown in Table S1.

Semi-quantitative RT-PCR was conducted using the KOD-Plus-Neo Kit (Toyobo) according to manufacturer's protocol. PCR was performed for 35 cycles at 94 °C for 30 s, 62 °C for 30 s, and 72 °C for X s (X = 10 s for ZIP2 exons 1–2, or 60 s for ZIP2 exons 1–4), or for 25 cycles at 94 °C for 30 s, 55 °C for 30 s, and 72 °C for 10 s (for GAPDH). The sequences of primers used for semi-quantitative RT-PCR are shown in Table S1.

2.4. Western Blotting and Slot Blotting Analysis

The protocol used for western blotting was previously reported (Suico et al., 2014; Sato et al., 2012). Western blots were probed with antibodies against ZIP2 (#ab99071; Abcam) and Hsc70 (#ADI-SPA-815; Enzo Life Sciences), followed by incubation with appropriate horseradish peroxidase-conjugated secondary antibodies. The Amersham ECL Western Blotting Detection Reagent (GE Healthcare) was used to visualize the blots.

MUC5AC protein secretion into the medium was detected by slot blotting. The protocol used was described previously (Nishimoto et al., 2010). An MUC5AC antibody was purchased from Thermo Fisher Scientific (#MA1-38223).

2.5. Flow Cytometric Analysis

Intracellular zinc was detected using Newport Green PDX acetoxymethyl ether (Thermo Fisher Scientific). Harvested cells (3×10^5 cells/mL) were washed twice with PBS and loaded with 1 μM Newport Green PDX acetoxymethyl ether for 15 min at 37 °C. Cells were washed by incubation in PBS for 30 min at 37 °C and then washed briefly 2 more times in PBS. These stained cells were analyzed using a JSAN Cell Sorter (Bay Bioscience). Data were analyzed using Flowlogic software (Miltenyi Biotec).

2.6. Measurement of Zinc Quantities

Zinc quantities in airway epithelial cells were measured using the Metalloassay Kit (Metallogenics), following the manufacturer's protocol. Absorbance was measured using an Epoch Microplate Spectrophotometer (BioTek).

2.7. Isc and ENaC Current Measurements

Isc values were measured in an Ussing chamber system following a previously described protocol (Caldwell et al., 2005). ENaC currents were measured using an EVOM volt–ohm meter (World Precision Instruments) following a previously described protocol (Sugahara et al., 2009).

2.8. Animal Experiments and Care

C57BL/6J-βENaC-Tg mice showed a CF-like pulmonary phenotype and were maintained as previously described (Shuto et al., 2016). Mouse tracheal surface epithelial cells from 11 to 13-week-old C57BL/6J-βENaC-Tg or WT C57BL/6J mice were harvested and cultured in air–liquid interface system as previously described (Ueno et al., 2008; Lu, 2004).

For intracellular zinc chelation *in vivo*, 10–14-week-old WT C57BL/6J male mice were intratracheally treated with 0.3 mg/kg TPEN dissolved in 10% DMSO in saline. Three hours later, mice were sacrificed to recover the right lung lobe for RNA isolation.

All mice were fed with normal chow ad libitum, and all procedures were approved in accordance with the guidelines of the animal facility center of Kumamoto University.

2.9. Gene-Expression Analysis Using a DNA Microarray

Total RNA was extracted from 16HBE14o-, βγENaC-16HBE14o-, NHBE, and DHBE-CF cells using the RNeasy Mini Kit (Qiagen), and samples were subjected to DNA-microarray analysis using the "3D-Gene" human oligo chip 24 k (Toray). The ratio (fold-induction) of gene-expression levels between 2 cell lines (16HBE14o- vs. βγENaC-16HBE14o- or NHBE vs. DHBE-CF) was measured based on the fluorescence intensities of Cy5 and Cy3, respectively. Differentially expressed genes, i.e., those with a log2 Cy3/Cy5 value of ≥2 or ≤ −2 (16HBE14o- vs. βγENaC-16HBE14o- cells) were clustered using Gene Cluster software (version 3.0, Stanford University) and viewed in a heatmap using Java TreeView software (version 1.1.6r4, Stanford University). GO biological-process term analysis of up-regulated genes (log2 ratio [Cy3/Cy5] ≥ 2) or down-regulated genes (log2 ratio [Cy3/Cy5] ≤ −2) in each comparison (16HBE14o- vs. βγENaC-16HBE14o-, NHBE vs. DHBE-CF, and βENaC-Tg mouse-derived lungs vs. WT mouse-derived lungs (Shuto et al., 2016)) was performed by GO-Term Finder (Lewis-Sigler Institute, Princeton University) (Boyle et al., 2004). Entries from the microarray data were approved by the Gene Expression Omnibus (GEO) and were assigned GEO accession numbers, GSE101829 (for human epithelial cells) and GSE101861 (for mouse lung tissue).

2.10. Statistical Analysis

The results are represented as the mean ± S.D. Differences among groups were analyzed by Student's *t*-test, or 1-way analysis of variance with Tukey's test or Dunnett's test (Statcel 3 program, OMS). P values < 0.05 were considered statistically significant. Trends (0.05 < P value ≤ 0.1) are also represented in the figures.

3. Results

3.1. Cellular and Molecular Biological Characterization of ENaC-Overexpressing Cells Link Hyperactive-ENaC and Defective-CFTR Conditions in Airway Epithelial Cells

Although defective-CFTR and hyperactive ENaC conditions are being considered as CF-like conditions, there is no study directly comparing these conditions from molecular and cellular aspects. Firstly, we sought to understand similarities between defective-CFTR and hyperactive-ENaC conditions in airway epithelial cells by characterizing the cellular and molecular biology of ENaC-overexpressing airway epithelial cells (βγENaC-16HBE14o- cells). Quantitative reverse transcriptase-polymerase chain reaction (RT-PCR) analysis of absolute copy numbers of mRNA transcripts encoding αENaC, βENaC, and γENaC revealed that CFTR-positive normal airway epithelial 16HBE14o- cells have higher mRNA levels of αENaC and lower levels of βENaC and γENaC, compared to parental 16HBE14o- cells (Fig. 1a, left). Overexpression of both βENaC and γENaC in 16HBE14o- cells resulted in higher levels of βENaC and γENaC relative expression compared with parental 16HBE14o- cells (Fig. 1b and c), which were comparable to the expression level of the αENaC transcript (Fig. 1a, right). ENaC overexpression promoted higher amiloride-sensitive ENaC channel activity after trypsin exposure in βγENaC-16HBE14o- cells (Fig. 1d and e).

To determine whether the gene-expression profile of βγENaC-16HBE14o- cells was similar to that of CFTR-defective CF airway epithelial cells, we performed DNA-microarray analysis using the "3D-Gene" Human Oligo chip 24 k (Toray Industries) and ratiometric analysis (fold-induction) of gene-expression levels between 16HBE14o- and βγENaC-16HBE14o- cells. Among the 24,460 genes probed in the chip, the expression levels of 339 genes were up-regulated (≥4-fold) and 147 genes were down-regulated (≤0.25-fold) in βγENaC-16HBE14o- cells (Fig. 1f, Table S2). Moreover, further DNA-microarray analysis using RNA samples isolated from primary normal human bronchial

Fig. 1. Association of cellular and molecular biological characteristics of ENaC-overexpressing cells with hyperactive-ENaC and defective-CFTR conditions in airway epithelial cells. (a–c) Total levels of α, β, and γENaC mRNA (a) and the relative expression levels of β and γENaC mRNA (b and c) in 16HBE14o- and βγENaC-16HBE14o- airway epithelial cells were measured by quantitative RT-PCR (n = 3). (d, e) Continuous recording of the amiloride-sensitive, short-circuit current (*Isc*) before and during apical exposure to trypsin (Try, 10 μg/mL). Apical amiloride (Ami, 100 μM) inhibited the current, as shown in βγENaC-16HBE14o- cells. (f, g) MA plot of the average gene-expression levels (log2) (x-axis) and mean fold-changes (log2) (y-axis) in 16HBE14o- and βγENaC-16HBE14o- cells (f), primary NHBE, and DHBE-CF cells (g). (h) Heat map representing the clusters of up-regulated (log2 ratio [Cy3/Cy5] ≥ 2.0) or down-regulated (log2 ratio [Cy3/Cy5] ≤ −2.0) genes in 16HBE14o- and βγENaC-16HBE14o- cells. (i) The patterns and numbers of genes in each cluster set of (h) are indicated. (j, k) Venn diagram of the overlaps of GO biological-process terms between 16HBE14o- vs. βγENaC-16HBE14o- cells and primary NHBE vs. DHBE-CF cells (j), and βENaC Tg vs. WT mouse-derived lungs (k). These GO biological-process terms were analyzed for up-regulated or down-regulated genes that showed a significant difference (log2 ratio Cy3/Cy5 ≥ 2.0 or ≤ −2.0) in each comparison. (l, m) Gene expression of MUC5AC in 16HBE14o-, βγENaC-16HBE14o- and CFBE41o- cells (l), and NHBE and DHBE-CF cells (m) were measured by quantitative RT-PCR (n = 3). (b, c, l, m) The values shown represent the mean ± SD. *p < 0.05, **p < 0.01, ***p < 0.005; Student's *t*-test.

epithelial (NHBE) cells from a healthy donor and diseased human bronchial epithelial cells from patients with CF (DHBE-CF) identified 658 up-regulated genes (≥4-fold) and 354 down-regulated genes (≤0.25-fold) in DHBE-CF cells (Fig. 1g, Table S3). Microarray-based cluster analysis was performed to ascertain which pathways were affected under ENaC-hyperactive and CFTR-defective conditions in airway epithelial cells. Six cluster sets were identified based on the gene-expression differences in both sets of paired airway epithelial cells (16HBE14o- vs.

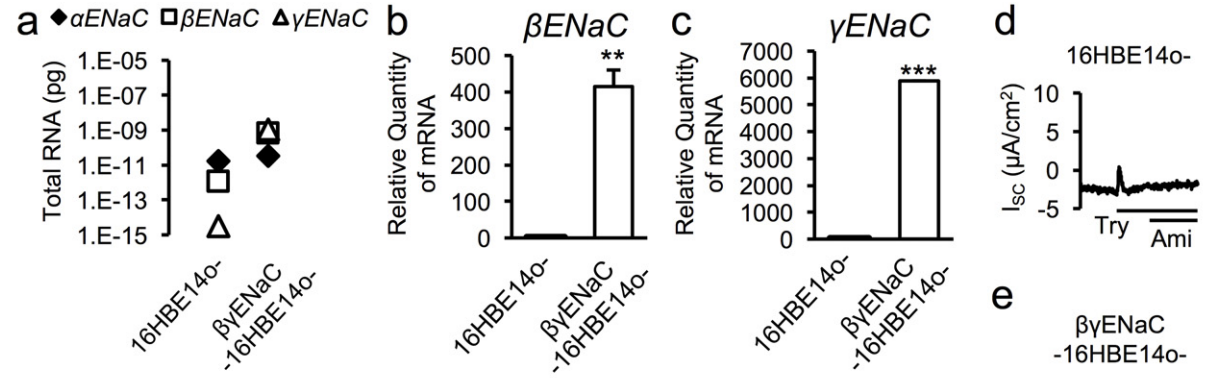

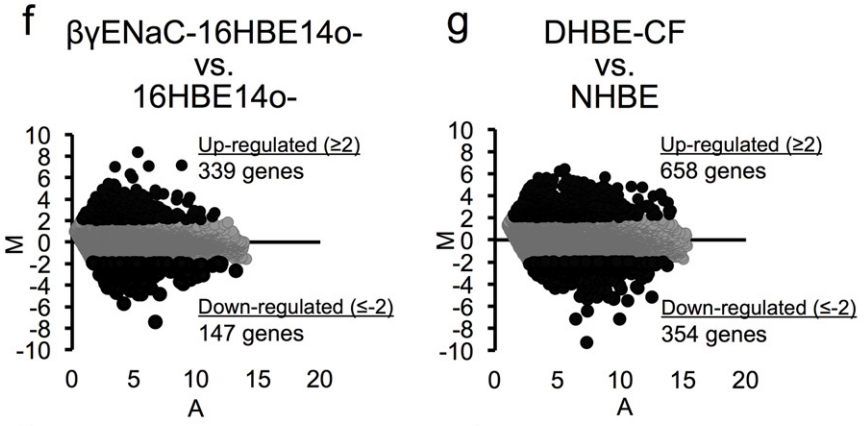

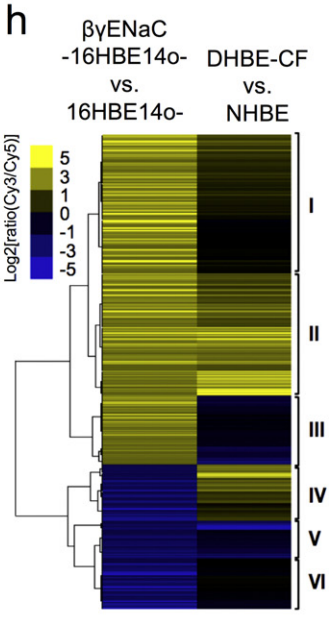

i

	βγENaC -16HBE14o- vs. 16HBE14o-	DHBE-CF vs. NHBE	# of Genes
Cluster I	+ +	± or +	127
Cluster II	+ +	+ +	111
Cluster III	+ +	± or -	63
Cluster IV	- -	+ or + +	52
Cluster V	- -	- or - -	34
Cluster VI	- -	±	46

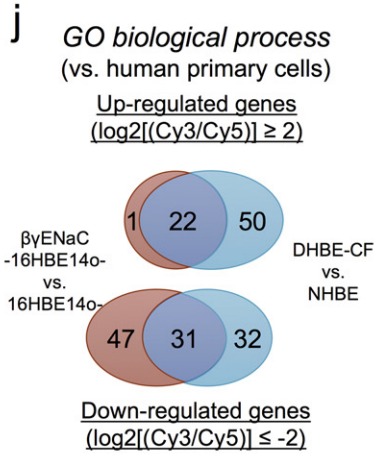

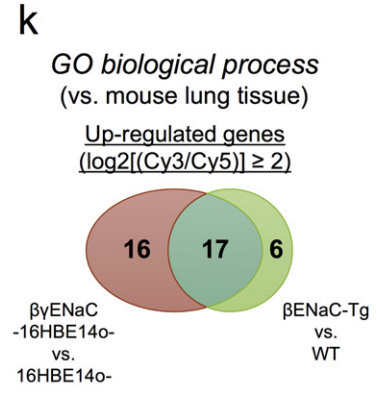

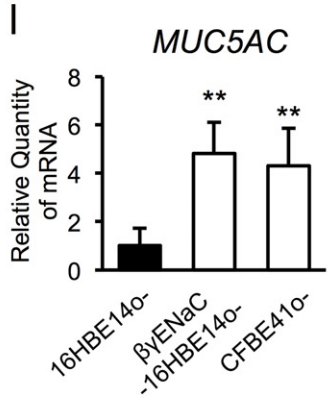

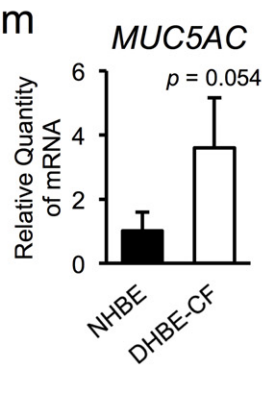

βγENaC-16HBE14o- and NHBE vs. DHBE-CF), as shown in Fig. 1h and Table S4. Genes in clusters II (111 genes) and V (34 genes) were significantly and similarly up- or down-regulated in both βγENaC-16HBE14o- and DHBE-CF cells, while genes in clusters I (127 genes), III (63 genes), and VI (46 genes) were significantly up- or down-regulated in βγENaC-16HBE14o- cells, but were not dramatically altered in DHBE-CF cells (Fig. 1i, Table S4). Genes in cluster IV (52 genes) were significantly down-regulated in βγENaC-16HBE14o- cells, but were up-regulated in DHBE-CF cells (Fig. 1i, Table S4). These cluster analyses demonstrated that approximately one fifth of differentially expressed genes in ENaC-hyperactive βγENaC-16HBE14o- cells (97 of 433 genes in clusters II and V) had similar gene-expression patterns to those in CFTR-defective DHBE-CF cells (Fig. 1i, Table S4). The genes in clusters II and V, such as *SAA1*, *SAA2*, *SAA4*, *S100A8*, *TLR3*, *FUT2*, *IL15*, *EPHX2*, *CYP24A1*, and *PTX3*, could be considered as both CFTR- and ENaC-sensitive genes. Gene ontology (GO) analysis revealed that half of the biological-process terms that were significantly represented in βγENaC-16HBE14o- cells (53 of 101 terms) were similarly altered in DHBE-CF cells (Fig. 1j, Table S5 and S6). These terms included inflammation, cell death, and protein phosphorylation. To clarify the *in vivo* relevance of the gene dysregulation observed in βγENaC-16HBE14o- cells, we focused on gene-expression profiles in the lung tissues of wild-type (WT) and βENaC-Tg mice (Shuto et al., 2016). Notably, 17 of 33 up-regulated GO biological process terms were similarly increased in the lung tissues of βENaC-Tg mice (Fig. 1k, Table S7). These data suggested that ENaC hyperactivation in airway epithelial cells mimicked, at least in part, the molecular environment in CF airway epithelial cells and of CF lung tissues.

Finally, in addition to the above-mentioned gene alterations, quantitative RT-PCR showed significant up-regulation of mucus hypersecretory marker gene, MUC5AC, a pathophysiologically relevant molecular marker in βENaC-Tg mouse lung tissues (Shuto et al., 2016), but not MUC5B, in ENaC-hyperactive βγENaC-16HBE14o- cells, as well as CFTR-defective CFBE41o- and primary DHBE-CF cells (Fig. 1l and m). Knockdown of βENaC expression in βγENaC-16HBE14o- cells down-regulated MUC5AC gene expression, implying that ENaC-dependent MUC5AC induction is reversible (Fig. S1). Together, our data confirm βγENaC-16HBE14o- cells as CF-like airway epithelial cells that can exhibit a mucus-hypersecretion phenotype, a typical characteristic of CF airway epithelial cells.

3.2. Down-Regulation of Intracellular Zinc Levels in CF and CF-Like Airway Epithelial Cells

Despite many recent reports showing regulatory roles of the zinc ion in controlling the expression levels of various genes (Jackson et al., 2008), its modulation in CF pathogenesis is unknown. To clarify whether zinc dysregulation is a feature of CF and CF-like airway epithelial cells, we measured zinc levels in the cell lysates of several airway epithelial cell lines, including normal 16HBE14o-, ENaC-hyperactive βγENaC-16HBE14o-, CFTR-defective CFBE41o- and CFTR-rescued CFBE41o- (WT-CFTR-CFBE41o-) cells. Importantly, statistically significant decreases in cellular zinc levels were observed in βγENaC-16HBE14o- and CFBE41o- cells (Fig. 2a). The free intracellular zinc levels were determined using the cell-permeable fluorophore Newport green, which further revealed that intracellular zinc levels were down-regulated in live βγENaC-16HBE14o- and CFBE41o- cells (Fig. 2b and c). Consistently, expression of the metallothionein 2A (MT2A) gene, a molecular marker of intracellular zinc levels, was also dampened in βγENaC-16HBE14o- and CFBE41o- cells (Fig. 2d). Notably, the levels of intracellular zinc and MT2A gene expression were significantly rescued by WT-CFTR complementation in CFBE41o- cells (Fig. 2a–d), suggesting the existence of a CFTR-dependent, zinc-regulatory mechanism. Taken together, these results confirm that CFTR-dependent and ENaC-dependent zinc deficiencies occur in CF and CF-like airway epithelial cells.

3.3. Intracellular Zinc Depletion Up-Regulates MUC5AC Expression in Normal Airway Epithelia

Because increased expression of the mucus-hypersecretion marker gene MUC5AC (Fig. 1l and m) and decreased intracellular zinc levels were common features in ENaC-hyperactive βγENaC-16HBE14o- cells, as well as CFTR-defective CFBE41o- and primary DHBE-CF cells (Fig. 2a–d), we next examined the possible relationship between intracellular zinc and MUC5AC expression in airway epithelial cells. Intracellular zinc depletion by *N, N, N, N′*-tetrakis (2-pyridyl-methyl) ethylenediamine (TPEN), a specific intracellular zinc chelator, consistently down-regulated the MT2A gene (a downstream target of zinc-dependent transcription) and up-regulated MUC5AC gene expression in normal airway epithelial 16HBE14o- cells, while these changes were rescued by zinc supplementation ($ZnCl_2$ addition) (Fig. 2e and f). Slot blotting analysis of cell-conditioned media further revealed that intracellular zinc depletion positively regulates MUC5AC secretion in airway epithelial cells (Fig. 2g and h). Finally, intratracheal instillation of TPEN in WT C57BL/6J mice showed induction of Muc5ac gene expression in airway tissues (Fig. 2i). Together, these results demonstrate that zinc depletion in airway epithelial cells is sufficient to increase mucin expression both *in vitro* and *in vivo*.

3.4. Down-Regulation of ZIP4, ZIP8, ZIP10, and ZIP14 Does Not Directly Contribute to CF-Associated MUC5AC Induction in Airway Epithelial Cells

Mammalian zinc transporter consists of 2 families: 14 members of the ZIP/SLC39A family and 10 members of the zinc exporter ZnT (zinc transporter; also known as SLC30A) family. Dysregulation of certain zinc transporters results in impaired zinc homeostasis and development of zinc-imbalance-related diseases, such as cancer, diabetes, osteoarthritis (Kim et al., 2014; Taylor et al., 2012; Tamaki et al., 2013). To identify critical zinc transporters that control CF-dependent intracellular zinc depletion, we first examined the mRNA-expression levels of several ZnTs and ZIPs, which were expected to be expressed in airway epithelial cells (Besecker et al., 2008), in non-CF and CF airway epithelial cells. Interestingly, quantitative RT-PCR analysis showed that some zinc transporter genes including (ZnT1, ZIP4, ZIP8, ZIP10, and ZIP14) were commonly down-regulated in both βγENaC-16HBE14o- and CFBE41o- cells (Fig. 3a). The fact that intracellular zinc levels are low in CF and CF-like airway epithelial cells prompted us to focus on the contribution of ZIP down-regulation in regulating MUC5AC expression. Small interfering RNA (siRNA)-based silencing of ZIP4, ZIP8, ZIP10, and ZIP14 showed that ZIP4 knockdown decreases intracellular zinc levels and that ZIP10 knockdown decreases MT2A expression (Fig. 3b and c, Fig. S2a–e). However, knocking down ZIP4 and ZIP10 had no effect on MUC5AC expression (Fig. 3d), suggesting that none of these ZIP transporters individually play an important role in zinc-dependent MUC5AC regulation. Moreover, simultaneous knockdown of 4 ZIP transporters (ZIP4, ZIP8, ZIP10, and ZIP14) also did not alter MUC5AC expression, despite decreases in the levels of intracellular zinc and MT2A expression (Fig. 3e–g, Fig. S2f–j), suggesting that downregulating these ZIP transporters in CF and CF-like airway epithelial cells does not directly contribute to CF-associated MUC5AC induction.

3.5. Identification of a Novel Splicing Variant of ZIP2 in CF and CF-Like Airway Epithelia and its Impact on ZIP2 Protein Expression

It was also important to clarify whether other intracellular zinc regulators relate to MUC5AC up-regulation in CF airway epithelial cells. Based on the increased ZIP2 gene-expression levels observed in CFBE41o- cells (Fig. 3a) and lung tissues from CF-like βENaC-Tg mice (Shuto et al., 2016), we next sought to examine the possible involvement of ZIP2 dysregulation in CF airway epithelial cells.

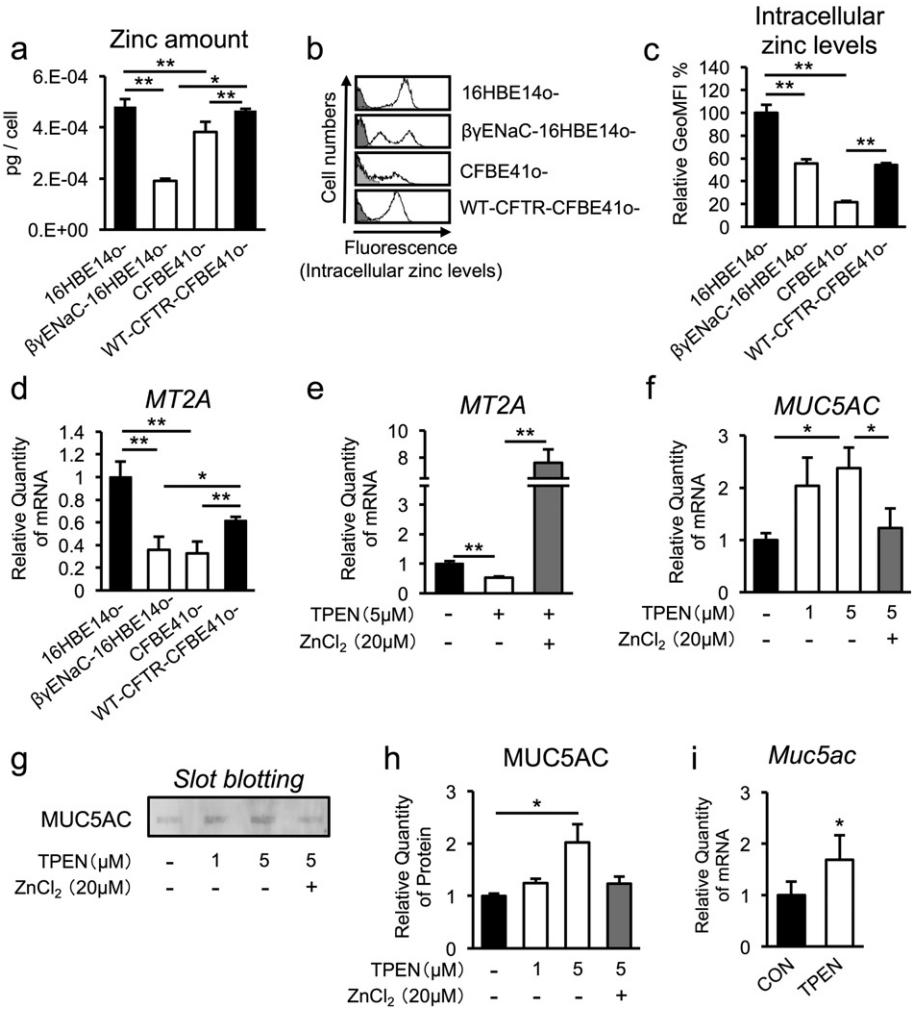

Fig. 2. Intracellular zinc down-regulation in CF and CF-like airway epithelia is important for MUC5AC up-regulation. (a) Total zinc volume of whole-cell components from normal (16HBE14o-), CF/CF-like (βγENaC-16HBE14o- and CFBE41o-), and WT-CFTR rescued CF (WT-CFTR- CFBE41o-) airway epithelial cells (n = 3). (b) Intracellular zinc levels in each airway epithelial cell line were measured by flow cytometry. The histograms show intracellular zinc-stained cells (white) and unstained cells (gray). (c) The relative geometric median fluorescence intensity (GeoMFI) of (b) is indicated (n = 3). (d) MT2A gene expression in each airway epithelial cell line was determined by quantitative RT-PCR (n = 3). (e, f) Gene-expression levels of MT2A (e) and MUC5AC (f) in 16HBE14o- cells treated with TPEN (1 or 5 μM) alone or concurrently with $ZnCl_2$ (20 μM) for 2 h were determined by quantitative RT-PCR (n = 3). (g) Secreted MUC5AC protein levels in culture medium from 16HBE14o- cells treated with TPEN (1 or 5 μM) alone or concurrently with $ZnCl_2$ (20 μM) for 6 h were determined by slot blotting. (h) Quantification of the bands shown in (g) (n = 3). (i) Gene expression of Muc5ac in whole lungs from male C57BL/6 J mice treated with vehicle (n = 5) and 0.3 mg/kg TPEN (n = 7) for 3 h was determined by quantitative RT-PCR. (a, c–f, h, i) The values shown represent the mean ± SD. *p < 0.05, **p < 0.01; Tukey's test (a, c–f, h), *p < 0.05; Student's t-test (i).

Western blotting analysis unexpectedly showed lower expression of the ZIP2 protein in βγENaC-16HBE14o- and CFBE41o- cells (Fig. 4a and b). To explain the discrepancy of ZIP2 expression at the mRNA and protein levels in airway epithelial cells, we next clarified whether a post-transcriptional regulatory mechanism is involved. Electrophoretic analysis of the full-length ZIP2 gene transcript revealed that a unique transcript approximately 200 base pairs longer than the normal ZIP2 gene-derived transcript is highly expressed in βγENaC-16HBE14o- and CFBE41o- cells (Fig. 4c). Sequence analysis confirmed the transcript as a novel splicing variant of ZIP2 that retains intron 1 between exons 1 and 2 of ZIP2 gene, which causes a frameshift that induces a premature stop codon (Fig. 4d and e). Because the splicing variant encoded a C-terminally deleted ZIP2 protein, the transcript was referred to as ΔC-ZIP2. Consistently, semi-quantitative RT-PCR analysis using a primer pair that amplified the mRNA sequence between exons 1 and 2 revealed that a lower WT-ZIP2 transcript amount (βγENaC-16HBE14o-, 0.34; CFBE41o-, 0.57; DHBE-CF, 0.33 vs. 16HBE14o-, 1.00; fold induction compared to the value of 16HBE14o- shown in Fig. 4f) and a higher ΔC-ZIP2 transcription ratio (out of total ZIP2 transcription; ΔC-ZIP2 + normal ZIP2) were a common feature in CF and CF-like airway epithelial cells (Fig. 4f and g). Moreover, quantitative RT-PCR analysis using ΔC-ZIP2 specific primers also confirmed that the amount of ΔC-ZIP2 transcript was higher in CF and CF-like airway epithelial cells (Fig. 4h and i), despite the fact that WT-ZIP2 per se was not induced (Fig. S3a and b). Complementation of WT-CFTR, but not mutant ΔF508-CFTR, increased the WT-ZIP2 amount and lowered the ΔC-ZIP2 expression ratio (Fig. 4j and k), implying that CFTR-dependent regulation of ΔC-ZIP2 production occurred. Notably, primary tracheal epithelial cells derived from CF-like βENaC-Tg mice also expressed an alternative-splicing transcript of mouse Zip2, which encodes an immature murine Zip2 protein due to the retention of intron 1 (Fig. 4l, Fig. S3c). Quantitative RT-PCR further confirmed higher expression of premature Zip2 transcript, with no alteration of WT-Zip2 transcript expression in βENaC-Tg mice-derived primary cells (Fig. S3d and e). Finally, to find out how a splicing switch from normal ZIP2 to ΔC-ZIP2 is induced in human CF airway epithelial cells, we extracted 4 relatively up- and down-regulated genes (up, ≥2-fold; down, ≤0.5-fold) that are known to be associated with splicing control, such as *IVNS1ABP*, *RNPC3*, *HNRNPH1*, and *U2AF1* genes

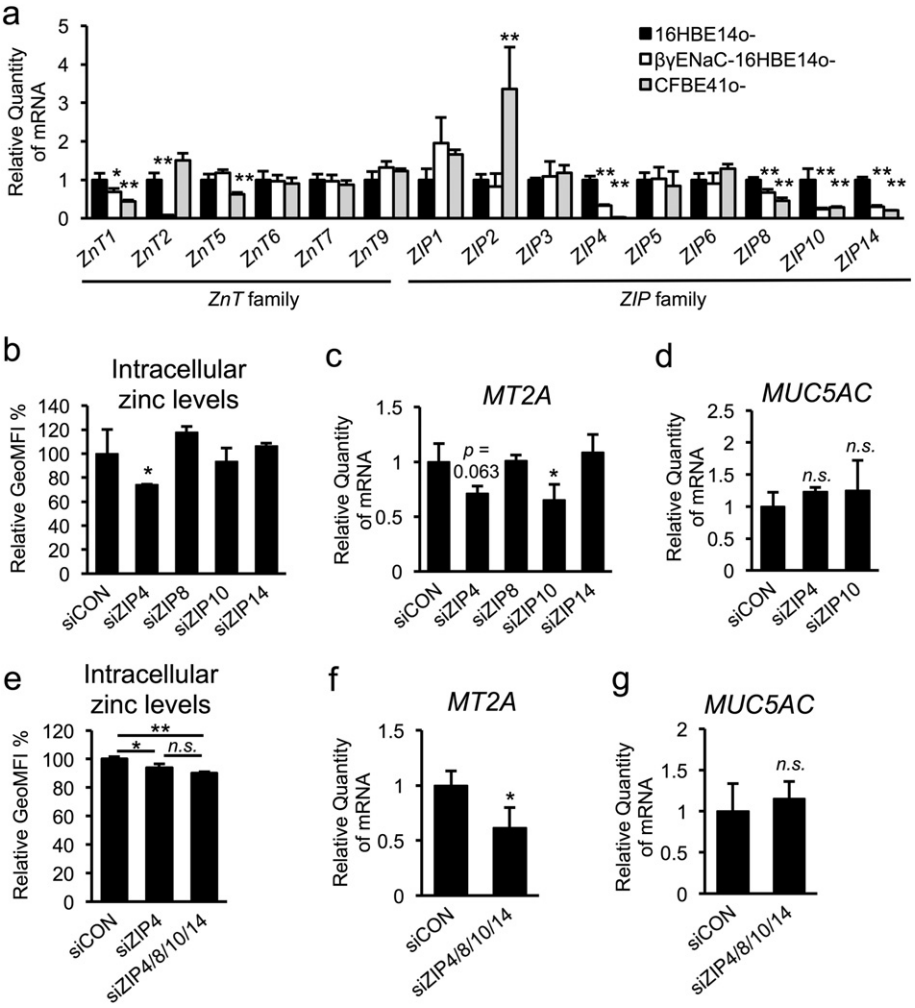

Fig. 3. Down-regulation of ZIP4, ZIP8, ZIP10, and ZIP14 do not contribute to CF-associated MUC5AC induction in airway epithelial cells. (a) Gene expression of ZnT- and ZIP-family members in normal (16HBE14o-) and CF/CF-like (βγENaC-16HBE14o- and CFBE41o-) airway epithelial cells was determined by quantitative RT-PCR (n = 3). (b–g) Normal airway epithelial cells (16HBE14o-) were transfected with ZIP4, ZIP8, ZIP10, or ZIP14 siRNA (50 nM) (b–d), or a mixture of each siRNA (25 nM) (e–g). (b, e) Intracellular zinc levels were measured by flow cytometry, and the relative GeoMFI is indicated (n = 3). (c, d, f, g) Gene-expression levels of MT2A (c and f) and MUC5AC (d and g) were determined by quantitative RT-PCR (n = 3). (a–g) The values shown represent the mean ± SD. *p < 0.05, **p < 0.01, *n.s.* (not significant); Dunnett's *t*-test (a–d). *p < 0.05, **p < 0.01, *n.s.* (not significant); Tukey's test (e). *p < 0.05, *n.s.* (not significant); Student's *t*-test (f, g).

(Table S3). Quantitative RT-PCR analysis revealed that *U2AF1B* gene, one of the three isoforms of *U2AF1* genes, was consistently down-regulated in CFTR-defective and ENaC-hyperactive cells, and other isoforms *U2AF1A* and *U2AF1C* were down-regulated in ENaC-hyperactive cells (Fig. S4a–f). However, siRNA-based knock down of *U2AF1* genes had no effects on ZIP2 splicing switch despite the relatively high knockdown efficiency of *U2AF1* genes (Fig. S4g–j). Together, our data show that CFTR-defective and ENaC-hyperactive airway epithelial cells induce a splicing switch from normal ZIP2 to ΔC-ZIP2 at least via U2AF1-independent mechanisms, presumably resulting in the production of a truncated ZIP2 protein.

3.6. ZIP2 Down-Regulation Accompanying a Decreased Expression of Other ZIPs is Crucial for Zinc Deficiency in CF and CF-Like Cells

To determine the pathophysiological relevance of ZIP2 dysregulation in CF and CF-like airway epithelial cells, we measured the effect of ZIP2 knockdown on the levels of intracellular zinc and MUC5AC expression.

Fig. 4. Identification of a novel splicing variant of ZIP2 in CF and CF-like airway epithelia and its impact on ZIP2 protein expression. (a) ZIP2 protein-expression levels in normal (16HBE14o-) and CF/CF-like (βγENaC-16HBE14o- and CFBE41o-) airway epithelial cells were assessed by western blotting. (b) Quantification of the bands shown in (a) (n = 3) (c) ZIP2 variants in normal (16HBE14o- and primary NHBE) and CF/CF-like (βγENaC-16HBE14o-, CFBE41o-, and primary DHBE-CF) airway epithelial cells were detected by PCR, using specific primers for the full-length ZIP2 mRNA transcript. (d) Sequence of human ΔC-ZIP2. Underlining indicates the exon 1 and exon 2 regions, and italic lettering shows the premature stop codon caused by the frameshift. (e) Schematic representation of human WT-ZIP2 and ΔC-ZIP2. (f) Gene expression of WT-ZIP2 and ΔC-ZIP2 in each cell line was determined by semi-quantitative RT-PCR. The relative intensity of PCR bands was quantified and indicated below the gel images. (g) The ΔC-ZIP2-expression ratio (relative to total ZIP2 expression) in (f) is indicated (n = 3). (h, i) Gene expression of ΔC-ZIP2 in cell lines (h) and primary cells (i) was determined by quantitative RT-PCR using primers targeting the ZIP2 intron 1 of ΔC-ZIP2 (n = 3). (j) Gene-expression levels of WT-ZIP2 and ΔC-ZIP2 in CF (CFBE41o-), WT-CFTR-rescued CF (WT-CFTR-CFBE41o-), and dysfunctional CFTR-induced CF (ΔF508-CFTR-CFBE41o-) were determined by semi-quantitative RT-PCR. The relative intensity of PCR bands was quantified and indicated below the gel images. (k) The ΔC-ZIP2 expression ratio (relative to total ZIP2 expression) in (j) is indicated (n = 3) (l) Gene-expression levels of Wt-zip2 and intron 1-retained Zip2 in primary airway epithelial cells isolated from WT and βENaC-Tg C57BL/6 J mice were determined by semi-quantitative RT-PCR. The relative intensity of PCR bands was quantified and indicated below the gel images. (b, g–i, k) The values shown represent the mean ± SD. *p < 0.05, **p < 0.01 (vs. 16HBE14o- cells), #p < 0.05 (vs. primary NHBE cells); Dunnett's *t*-test (b, g, h). *p < 0.05; Student's *t*-test (i). *p < 0.05, *n.s.* (not significant) (vs. CFBE41o- cells); Dunnett's *t*-test (k).

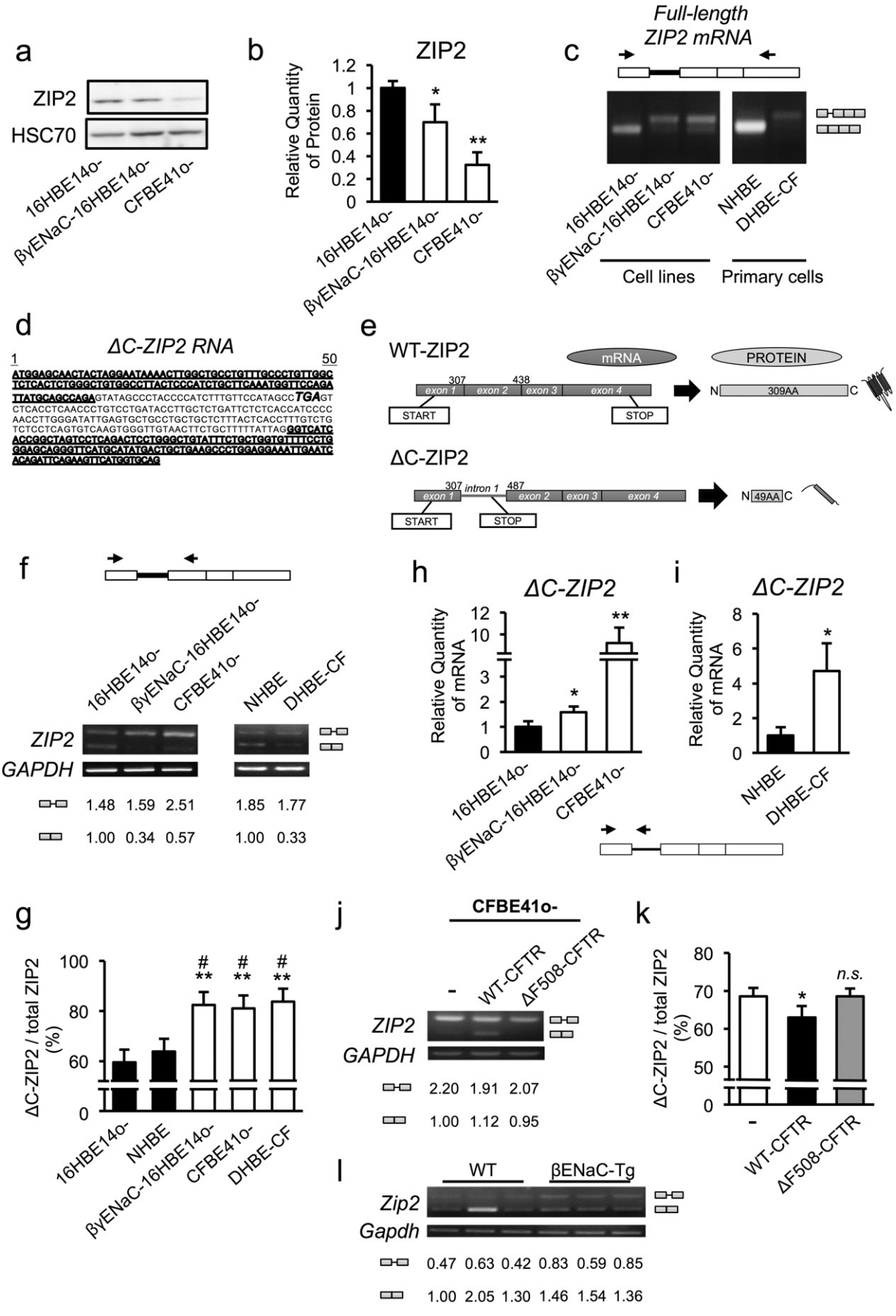
a
ZIP2
HSC70
16HBE14o-
βγENaC-16HBE14o-
CFBE41o-
b
ZIP2
Relative Quantity of Protein
1.2
1
0.8
0.6
0.4
0.2
0
*
**
16HBE14o-
βγENaC-16HBE14o-
CFBE41o-
c
Full-length ZIP2 mRNA
16HBE14o-
βγENaC-16HBE14o-
CFBE41o-
NHBE
DHBE-CF
Cell lines
Primary cells
d
ΔC-ZIP2 RNA
1
50
ATGGAGCAACTACTAGGAATAAAACTTGGCTGCCTGTTTGCCCTGTTGGC
TCTCACTCTGGGCTGTGGCCTTACTCCCATCTGCTTCAAATGGTTCCAGA
TTATGCAGCCAGAGTATAGCCCTACCCCATCTTTGTTCCATAGCCTGAGT
CTCACCTCAACCCTGTCCTGATACCTTGCTCTGATTCTCTCACCATCCCC
AACCTTGGGATATTGAGTGCTGCCTGCTGCTCTTTACTCACCTTTGTCTG
TCTCCTCAGTGTCAAGTGGGTTGTAACTTCTGCTTTTTATTAGGGTCATC
ACCGGCTAGTCCTCAGACTCCTGGGCTGTATTTCTGCTGGTGTTTTCCTG
GGAGCAGGGTTCATGCATATGACTGCTGAAGCCCTGGAGGAAATTGAATC
ACAGATTCAGAAGTTCATGGTGCAG
e
WT-ZIP2
mRNA
PROTEIN
307
438
exon 1
exon 2
exon 3
exon 4
START
STOP
N
309AA
C
ΔC-ZIP2
307
intron 1
487
exon 1
exon 2
exon 3
exon 4
START
STOP
N
49AA
C
f
16HBE14o-
βγENaC-16HBE14o-
CFBE41o-
NHBE
DHBE-CF
ZIP2
GAPDH
1.48 1.59 2.51 1.85 1.77
1.00 0.34 0.57 1.00 0.33
h
ΔC-ZIP2
Relative Quantity of mRNA
12
10
3
2
1
0
*
**
16HBE14o-
βγENaC-16HBE14o-
CFBE41o-
i
ΔC-ZIP2
Relative Quantity of mRNA
8
6
4
2
0
*
NHBE
DHBE-CF
g
ΔC-ZIP2 / total ZIP2 (%)
100
80
60
0
**
**
**
16HBE14o-
NHBE
βγENaC-16HBE14o-
CFBE41o-
DHBE-CF
j
CFBE41o-
-
WT-CFTR
ΔF508-CFTR
ZIP2
GAPDH
2.20 1.91 2.07
1.00 1.12 0.95
k
ΔC-ZIP2 / total ZIP2 (%)
80
70
60
50
0
*
n.s.
-
WT-CFTR
ΔF508-CFTR
l
WT
βENaC-Tg
Zip2
Gapdh
0.47 0.63 0.42 0.83 0.59 0.85
1.00 2.05 1.30 1.46 1.54 1.36

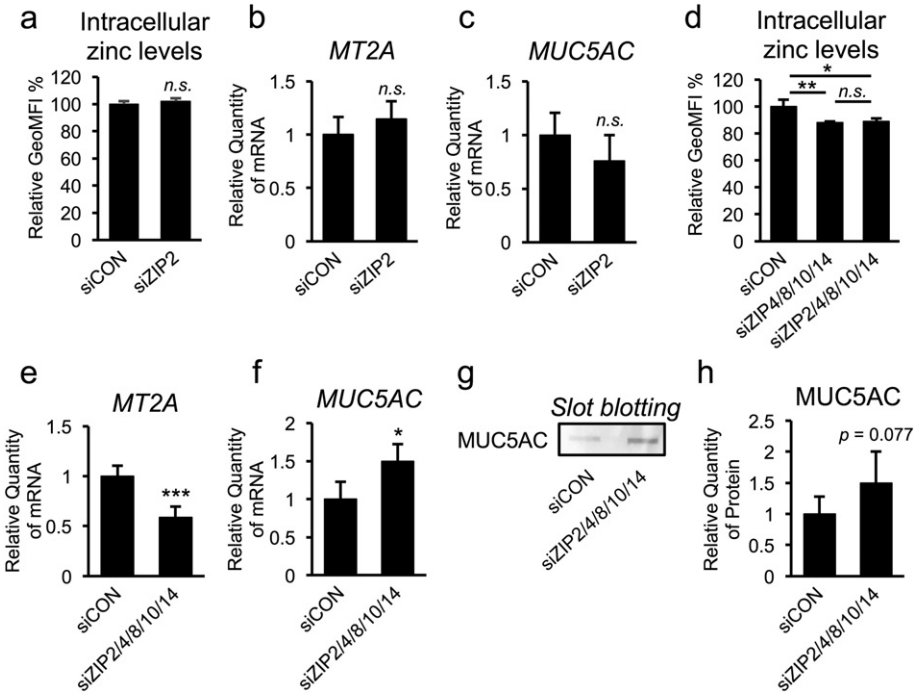

Fig. 5. ZIP2 is a key regulator that restricts MUC5AC up-regulation in airway epithelial cells. (a–h) Normal airway epithelial cells (16HBE14o-) were transfected with ZIP2 siRNA (50 nM) (a–c); a ZIP4, ZIP8, ZIP10, and ZIP14 siRNA mixture (25 nM each siRNA) (d); and a ZIP2, ZIP4, ZIP8, ZIP10, and ZIP14 siRNA mixture (25 nM each siRNA) (d–h). (a, d) Intracellular zinc levels were measured by flow cytometry and the relative GeoMFI is indicated (n = 3). (b, c, e, f) Gene-expression levels of MT2A (b and e) and MUC5AC (c and f) were determined by quantitative RT-PCR (b and c, n = 3; e and f, n = 4). (g) Secreted protein expression of MUC5AC was determined by slot blotting. (h) Quantification of the bands shown of (g) was quantified (n = 4). (a–f, h) The values shown represent the mean ± SD. *p < 0.05, ***p < 0.005, *n.s.* (not significant); Student's t-test (a–c, e, f, h). *p < 0.05, **p < 0.01, *n.s.* (not significant); Tukey's test (d).

Like most of the ZIP transporters, reducing ZIP2 expression alone had no effect on intracellular zinc levels, MT2A expression, or MUC5AC expression in non-CF airway epithelial cells (Fig. 5a–c, Fig. S5a and b). Importantly, however, knockdown of ZIP2 together with a quartet of other ZIPs (ZIP4, 8, 10, and 14) significantly reduced intracellular zinc levels and MT2A expression (Fig. 5d and e, Fig. S5c–S5h), and significantly induced MUC5AC expression at both the mRNA and protein levels (Fig. 5f–h). Because knockdown of the ZIP quartet alone had no impact on MUC5AC expression (Fig. 3g), ZIP2 down-regulation accompanying a decreased expression of other ZIPs is crucial for zinc deficiency in CF and CF-like cells. The results further support the idea of splice switch from WT-ZIP2 to ΔC-ZIP2 as a key restriction step that accelerates MUC5AC up-regulation in airway epithelial cells through orchestration with other ZIP transporters.

3.7. Characterization of the ΔC-ZIP2 Protein

Although the splice switch-dependent reduction of functional WT-ZIP2 expression may play a crucial role in CF pathogenesis, a possible direct involvement of ΔC-ZIP2 protein-mediated in such a mechanism could not be ruled out. To test this possibility, we characterized the effect of exogenously ΔC-ZIP2 protein expression in HSG cells, a human submandibular gland cell line with high transfection efficiency. Western blot analysis confirmed successful transfection of the His/Myc-tagged WT-ZIP2 and ΔC-ZIP2 genes (Fig. S6a and b). Overexpression of WT-ZIP2, but not ΔC-ZIP2, increased both intracellular zinc levels and MT2A expression (Fig. S6c–e), suggesting that ΔC-ZIP2 has no zinc-importing activity. Cellular fractionation and immunofluorescence analyses revealed that WT-ZIP2 localizes at the plasma membrane, while ΔC-ZIP2 accumulates in the membrane fraction (Fig. S6f) and possibly at the endoplasmic reticulum (ER)/Golgi-associated membrane, but not at the plasma membrane. (Fig. S6g). These results demonstrate that the ΔC-ZIP2 protein was stably expressed, although it did not localize to the plasma membrane and has no zinc-importing activity.

3.8. ΔC-ZIP2 Specifically Up-Regulates βENaC Gene Expression in a Zinc-Independent Manner

To determine a direct role of ΔC-ZIP2 in CF airway pathogenesis, we examined the effect of ΔC-ZIP2 overexpression in normal 16HBE14o- cells. Stable transduction with a lentiviral vector encoding the full-length intact ΔC-ZIP2 sequence (exon 1 + intron 1 + the other exons) in 16HBE14o- cells unexpectedly showed expression of the full-length, intact WT ZIP2 protein (exon 1 + other exons), but not the ΔC-ZIP2 protein, implying that correct splicing occurs under this condition (ΔC-ZIP2, Fig. 6a–c). To suppress the endogenous splicing reaction, we next established the vector coding ΔC-ZIP2 sequence with an intronic mutation (IVS1 + T > C) to produce a variant with an unspliceable intron 1. Importantly, a stable transduction harboring the full-length ΔC-ZIP2 (IVS1 + T > C) variant expressed only the ΔC-ZIP2 transcript (IVS1 + T > C ΔC-ZIP2, Fig. 6b and c) and had no effect on endogenous ZIP2 protein expression (Fig. 6d and e), indicating that ΔC-ZIP2 does not exert a dominant-negative effect. To next examine the role of ΔC-ZIP2 in regulating CF-associated gene expression, we performed quantitative RT-PCR analyses in ΔC-ZIP2 (IVS1 + T > C)-expressing 16HBE14o- cells. Consistently, MT2A expression was not affected by ΔC-ZIP2 transfection, confirming that ΔC-ZIP2 per se does not have any zinc-importing activity (Fig. 6f). Notably, ΔC-ZIP2 transfection did not affect most CF-associated gene-expression levels, except for βENaC (Fig. 6g). Accordingly, ZIP2 knockdown attenuated βENaC transcription (Fig. S7a and b). Moreover, ΔC-ZIP2 introduction slightly up-regulated ENaC channel activity, consistent with the effect on βENaC mRNA (Fig. 6h). ΔC-ZIP2 with an early stop codon mutation (K8X), whose protein product reflects truncation of most of the protein-coding region, did not induce βENaC gene expression; thus, the ΔC-ZIP2 variant was responsible for βENaC up-regulation

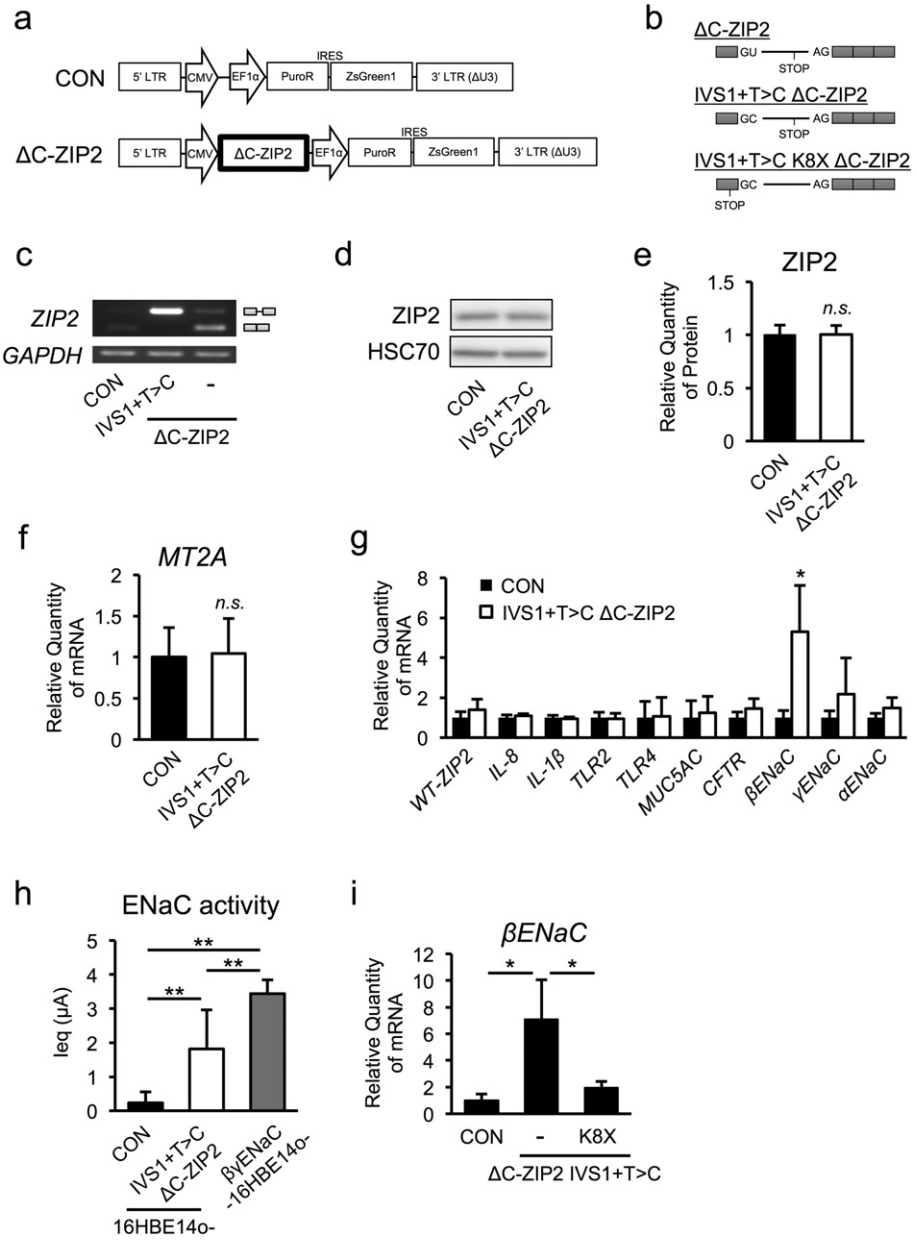

Fig. 6. ΔC-ZIP2 specifically up-regulates βENaC gene expression in a zinc-independent manner. (a, b) Schematic representation of lentiviral constructs (a) and full-length ZIP2 or ΔC-ZIP2 (b) (c) ZIP2 mRNA splicing in the WT gene and non-splice mutant (IVS1 + T > C) ΔC-ZIP2, stable expressed in 16HBE14o- cells, was determined by PCR. (d) ZIP2 protein in 16HBE14o- cells stably expressing IVS1 + T > C ΔC-ZIP2 was assessed by western blotting. (e) The intensities of the bands shown in (d) were quantified (n = 3). (f, g) Expression of the MT2A gene (f) and CF-associated genes (g) in 16HBE14o- cells stably expressing IVS1 + T > C ΔC-ZIP2 were determined by quantitative RT-PCR (n = 3). (h) Amiloride-sensitive equivalent currents (Ieq) in 16HBE14o- cells stably expressing IVS1 + T > C ΔC-ZIP2 and βγENaC-16HBE14o- were detected as the ENaC current (n = 6). (i) Gene-expression levels of βENaC in 16HBE14o- cells stably expressing IVS1 + T > C ΔC-ZIP2 and an early-truncated (K8X) IVS1 + T > C ΔC-ZIP2 variant were determined by quantitative RT-PCR (n = 3). (e–i) The values shown represent the mean ± SD. *p < 0.05, *n.s.* (not significant); Student's t-test (e–g). *p < 0.05, **p < 0.01; Tukey's test (h, i).

(Fig. 6i). Finally, we identified that p38, one of the key kinases critical for βENaC expression, is activated byΔC-ZIP2 expression in 16HBE14o- cells (Fig. S7c). However, p38 inhibition did not affect ΔC-ZIP2-dependent βENaC up-regulation (Fig. S7d). Overall, although a direct connection between βENaC expression and ENaC function is unclear, our data indicate that the ΔC-ZIP2 transcript-derived ΔC-ZIP2 protein may positively regulate ENaC function by possibly inducing βENaC gene expression (a key characteristic of CF pathogenesis) via an unknown zinc-independent mechanism.

4. Discussion

The present study reveals that CFTR-defective and/or ENaC-hyperactive conditions accelerated the conversion from WT-ZIP2 to ΔC-ZIP2 transcripts in airway epithelial cells, which potentially reduced the availability of plasma membrane-localized WT-ZIP2 protein, while increasing ER/Golgi-membrane localization of the ΔC-ZIP2 protein. The splice switch-dependent functional ZIP2 down-regulation as well as other ZIPs down-regulation are responsible for zinc deficiency in CF and CF-like cells (Fig. 7). Because lower intracellular Zn^{2+} levels contribute to CF-associated MUC5AC hypersecretion in airway epithelial cells, these findings uniquely link splice switching in ZIP2 and CF-associated MUC5AC induction. Generally, appropriate MUC5AC expression contributes to host defenses as a main component of mucociliary clearance (Ehre et al., 2012), but its overexpression, especially under airway clearance-defective conditions observed in CF airways, is thought to be an exacerbating factor for CF lung diseases (Henke et al., 2007; Groneberg et al., 2002; Kreda et al., 2012). Thus, identification

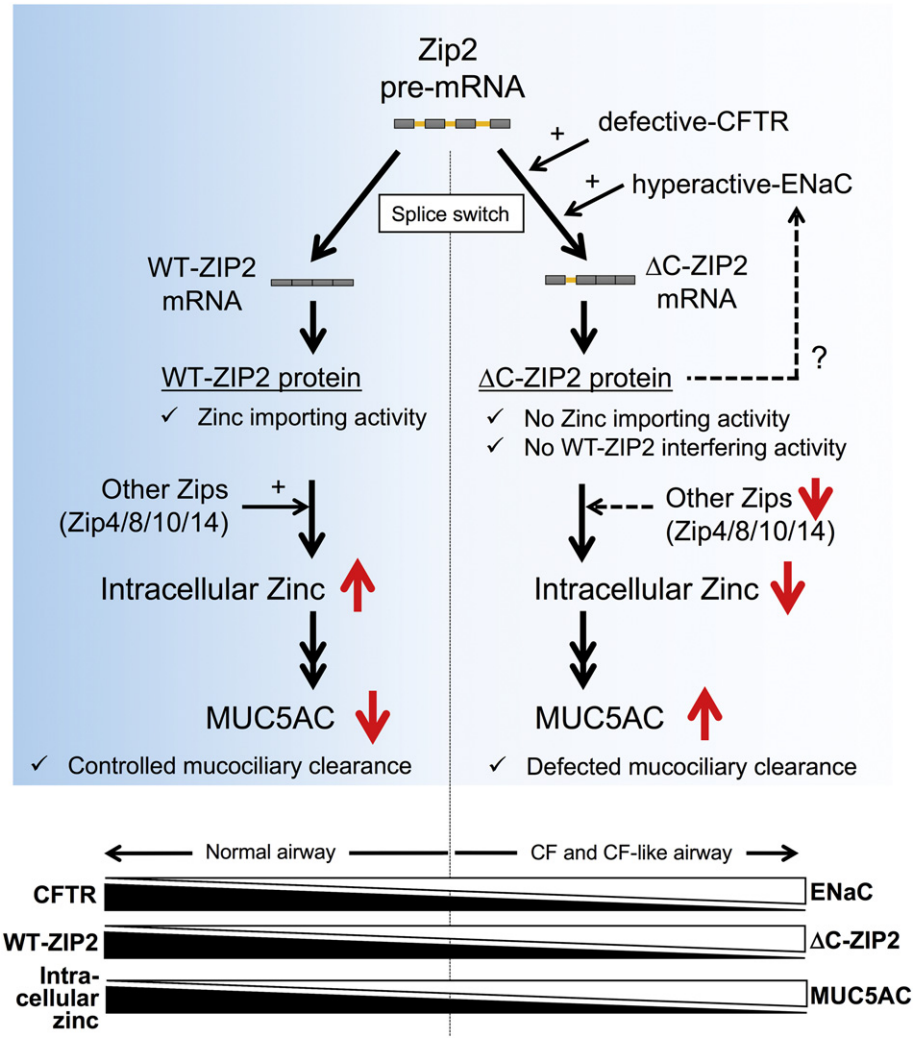

Fig. 7. Putative mechanisms of zinc deficiency-dependent MUC5AC hypersecretion in CF airway epithelial cells. In normal and non-CF airway epithelial cells (left panel), WT-ZIP2 mRNA-derived WT-ZIP2 and other ZIP proteins contribute to maintain intracellular zinc levels, resulting in the proper expression of mucin MUC5AC expression. In CF airway epithelial cells (right panel), splice switch from WT-ZIP2 to ΔC-ZIP2, an alternative splice isoform of ZIP2, which lacks the C-terminal domain, contributes to the down-regulation of functional WT-ZIP2 protein. ΔC-ZIP2 protein has no effects on zinc-importing and WT-ZIP2-interfering activities; thus, splice switch to ΔC-ZIP2 as well as down-regulation of other ZIPs causes intracellular zinc depletion in CF airway epithelial cells, which is sufficient to up-regulate MUC5AC expression. In the meantime, the ΔC-ZIP2 transcript-derived ΔC-ZIP2 protein likely positively regulates ENaC function by possibly inducing βENaC gene expression (a key characteristic of CF pathogenesis) *via* an unknown zinc-independent mechanism. Overall, the balance of CFTR and ENaC, and WT-ZIP2 and ΔC-ZIP2, affects intracellular zinc levels, which control MUC5AC secretion in airway epithelial cells.

of the molecules and pathways underlying CF-associated MUC5AC induction has been the subject of extensive research for many years (Imamura et al., 2004; Kang et al., 2015; Kreda et al., 2012). In this regard, our findings on the importance of Zn^{2+} and splice switch of its transporters could be instructive for exploring CF-associated mucus overproduction *in vitro*.

Alternative splicing is a well-characterized mechanism by which multiple transcripts are generated from a single immature mRNA sequence, which affects various functions in cellular processes, tissue specificity and developmental states (Wang et al., 2008; Luco et al., 2011). Dysregulation of alternative splicing can accelerate or attenuate the development of certain diseases (Cáceres and Kornblihtt, 2002; Cooper et al., 2009), indicating that its regulation could be pathophysiologically relevant. Importantly, most diseases resulting from alternative splicing are caused by change of splicing efficiency due to mutations in splicing-associated sequences in the corresponding genes (Cooper et al., 2009; Cáceres and Kornblihtt, 2002). In contrast, we identified a novel pathologically relevant splicing product of ZIP2, or ΔC-ZIP2, which was induced by CFTR-defective and/or ENaC-hyperactive conditions. Because a similar inducible splicing-switch system has only been described in ER stress-induced mRNA splicing to date (Ron and Hubbard, 2008; Kaufman, 2002), our study may strongly impact the field of alternative splicing-associated transcriptional regulation.

Identification of ZIP2 as one of the critical transporters responsible for CF-associated basal MUC5AC induction provides new insight into the regulation of airway mucus homeostasis. Reports on the functional expression of zinc transporters in airway epithelial cells have been limited to a few zinc transporter family members. Lang et al. showed increased ZIP1 and ZIP14 expression and decreased ZIP4 and ZnT4 expression during acute inflammation (Lang et al., 2007). Besecker et al. found that ZIP8 is induced after TNFα exposure (Besecker et al., 2008). In both cases, the intracellular Zn^{2+} levels regulated by these transporters were considered to protect the lungs from inflammation by activating several signaling molecules, such as PI3K and NF-κB (Bao, 2005; Liu et al., 2013). However, the role of ZIP2 has been mainly described in other tissues (not in airway epithelial cells), including pericentral hepatocytes, keratinocytes, and pulmonary macrophage, as well as in prostate cancer (Peters et al., 2007; Inoue et al., 2014; Hamon et al., 2014). It should be noted, though, that Roscioli et al. confirms ZIP2 expression in airway epithelial cells, and its expression is reduced by cigarette smoke exposure, accompanied with diminished

intracellular Zn^{2+} levels (Roscioli et al., 2017). Accordingly, our data also demonstrated that ZIP2 expression in airway epithelial cells and that ZIP2 dysregulation mainly contributes to CF-associated mucus overproduction, but careful interpretation may be needed. In fact, involvement of ZIP2 in the regulation of MUC5AC was only observed when its knockdown is performed together with other ZIPs. Because knockdown of a quartet of other ZIPs or of ZIP2 alone had no effect on MUC5AC expression, there may be functionally relevant interplay among ZIP transporters in the regulation of MUC5AC, for which ZIP2 plays a central role.

Physiological relevance and mechanism of ΔC-ZIP2-dependent ENaC activation is also an interesting issue. This could be considered as a feedforward CF-exacerbating pathway. But, whether ΔC-ZIP2-dependent βENaC mRNA up-regulation is responsible for ENaC activation is undetermined. From a different perspective, ΔC-ZIP2 may directly stabilize in part the ENaC expression itself at protein level, or affect ENaC-modulating proteins to indirectly stabilize ENaC protein expression. These "functional" roles of ΔC-ZIP2 in the regulation of CF lung pathogenesis will be explored in the future.

In clinical point of view, subjects including CF patients exhibiting low plasma Zn^{2+} levels (<90 μg/dL) are more susceptible to infections and tend to have higher levels of plasma oxidative stress molecules and inflammatory cytokines (Prasad et al., 2007; Mocchegiani et al., 1995), indicating the indispensable role of plasma zinc in the control of inflammation. Consistently, two clinical reports showed that zinc supplementation is beneficial to CF patients in the aspects of energy intake as well as infection episode and anti-inflammatory function (Van Biervliet et al., 2008; Abdulhamid et al., 2008). However, it should be noted that plasma zinc-adequate CF patients (101 ± 9.8 μg/dL, range 90–125 μg/dL) had lesser responses to zinc supplementation (Abdulhamid et al., 2008), suggesting that plasma Zn^{2+} levels restrict the efficiency of zinc supplement approach. On the other hand, our data clearly showed intracellular zinc deficiency as well as MUC5AC up-regulation as common characteristics in CF and mimicking low Zn^{2+} levels in CF and CF-like airway epithelial cells, achieved by TPEN treatment and siRNA-based knockdown of ZIP transporters, resulted in MUC5AC up-regulation, indicating that not plasma but intracellular zinc in airway is sufficient for CF-associated MUC5AC induction. Together, our data unveil a previously unknown connection between intracellular Zn^{2+} and mucus production at the cellular level of CF airways, and provide a novel concept that control of ZIP2 splice switch could be another target in the clinical use of Zn^{2+} in CF patients.

Funding Sources

This work was supported by the Japan Society for the Promotion Science (JSPS) KAKENHI (Grant Numbers JP25460102 and JP17H03570 (to T.S.), and JP15J09420 (to S.K.), the JSPS Program on Strategic Young Researcher Overseas Visits Program for Accelerating Brain Circulation (Grant Number S2510 [to H.K.]), and the Program for Leading Graduate Schools HIGO (Health life science: Interdisciplinary and Glocal Oriented; MEXT, Japan).

Conflict of Interest

The authors declare that they have no conflict of interest.

Author Contributions

S.K., H.K., and T.S. designed the research. S.K., H.F., H.N., K·U-S., K.M., C.M., Y.S., T.O., R.C.B., D.C.G., and T.S. performed the research and analyzed the data. S.K., H.F., H.N., K·U-S., K.M., R.N., T.K., C.M., Y.S., T.O., T.T., N.N., and T.S. contributed to the mouse production. S.K., M.A.S., J.D.L., H.K., and T.S. wrote the paper. T.S. and H.K. supervised the project.

Acknowledgments

We thank Dr. Ray A. Caldwell (University of North Carolina, Chapel Hill), Dr. Kazutsune Harada (Ono Pharmaceutical Company, Ltd.), Mr. Kazuhiko Higurashi (Shino-Test Corporation, Ltd.), and Dr. Hiromitsu Iwata (Nagoya Proton Therapy Center) for providing useful technical advice and assistance. We thank Editage [http://www.editage.com] for editing and reviewing this manuscript for English language.

Appendix A. Supplementary data

Supplementary data to this article can be found online at https://doi.org/10.1016/j.ebiom.2017.12.025.

References

Abdulhamid, I., et al., 2008. Effect of zinc supplementation on respiratory tract infections in children with cystic fibrosis. Pediatr. Pulmonol. 43 (3), 281–287.
Almaça, J., et al., 2013. High-content siRNA screen reveals global ENaC regulators and potential cystic fibrosis therapy targets. Cell 154 (6), 1390–1400.
Andreini, C., et al., 2006. Counting the zinc-proteins encoded in the human genome. J. Proteome Res. 5 (1), 196–201.
Astrand, A.B.M., et al., 2015. Linking increased airway hydration, ciliary beating, and mucociliary clearance through ENaC inhibition. Am. J. Physiol. Lung Cell. Mol. Physiol. 308 (1), L22–L32.
Bao, S., 2005. Zinc modulates airway epithelium susceptibility to death receptor-mediated apoptosis. Am. J. Physiol. Lung Cell. Mol. Physiol. 290 (3), L433–L441.
Besecker, B., et al., 2008. The human zinc transporter SLC39A8 (Zip8) is critical in zinc-mediated cytoprotection in lung epithelia. Am. J. Physiol. Lung Cell. Mol. Physiol. 294 (6), L1127–L1136.
Boucher, R.C., 2007. Cystic fibrosis: a disease of vulnerability to airway surface dehydration. Trends Mol. Med. 13 (6), 231–240.
Boyle, E.I., et al., 2004. GO::TermFinder - open source software for accessing gene ontology information and finding significantly enriched gene ontology terms associated with a list of genes. Bioinformatics 20 (18), 3710–3715.
Cáceres, J.F., Kornblihtt, A.R., 2002. Alternative splicing: multiple control mechanisms and involvement in human disease. Trends Genet. 18 (4), 186–193.
Caldwell, R.A., Boucher, R.C., Stutts, M.J., 2005. Neutrophil elastase activates near-silent epithelial Na+ channels and increases airway epithelial Na+ transport. Am. J. Physiol. Lung Cell. Mol. Physiol. 288 (5), L813–L819.
Cooper, T.A., Wan, L., Dreyfuss, G., 2009. RNA and disease. Cell 136 (4), 777–793.
Cozens, A.L., et al., 1992. Characterization of immortal cystic fibrosis tracheobronchial gland epithelial cells. Proc. Natl. Acad. Sci. U. S. A. 89 (11), 5171–5175.
Cozens, A.L., et al., 1994. CFTR expression and chloride secretion in polarized immortal human bronchial epithelial cells. Am. J. Respir. Cell Mol. Biol. 10 (1), 38–47.
Damphousse, V., et al., 2014. Plasma zinc in adults with cystic fibrosis: correlations with clinical outcomes. J. Trace Elem. Med. Biol. 28 (1), 60–64.
Duce, J.A., et al., 2010. Iron-export ferroxidase activity of β-amyloid precursor protein is inhibited by zinc in Alzheimer's disease. Cell 142 (6), 857–867.
Ehre, C., et al., 2012. Overexpressing mouse model demonstrates the protective role of Muc5ac in the lungs. Proc. Natl. Acad. Sci. U. S. A. 109 (41), 16528–16533.
Elborn, J.S., 2016. Cystic fibrosis. Lancet 388 (10059), 2519–2531.
Fukada, T., et al., 2011. Zinc homeostasis and signaling in health and diseases. J. Biol. Inorg. Chem. 16 (7), 1123–1134.
Grattan, B.J., Freake, H.C., 2012. Zinc and cancer: implications for LIV-1 in breast cancer. Nutrients 4 (7), 648–675.
Gray, R.D., et al., 2010. Sputum trace metals are biomarkers of inflammatory and suppurative lung disease. Chest 137 (3), 635–641.
Groneberg, D.A., et al., 2002. Expression of MUC5AC and MUC5B mucins in normal and cystic fibrosis lung. Respir. Med. 96 (2), 81–86.
Hamon, R., et al., 2014. Zinc and zinc transporters in macrophages and their roles in efferocytosis in COPD. PLoS One 9 (10), e110056.
Haq, I.J., et al., 2016. Airway surface liquid homeostasis in cystic fibrosis: pathophysiology and therapeutic targets. Thorax 71 (3), 284–287.
Hara, T., et al., 2017. Physiological roles of zinc transporters: molecular and genetic importance in zinc homeostasis. J. Physiol. Sci. 67 (2), 283–301.
Henke, M.O., et al., 2007. MUC5AC and MUC5B mucins increase in cystic fibrosis airway secretions during pulmonary exacerbation. Am. J. Respir. Crit. Care Med. 175 (8), 816–821.
Illek, B., et al., 2008. Cl transport in complemented CF bronchial epithelial cells correlates with CFTR mRNA expression levels. Cell. Physiol. Biochem. 22 (1–4), 57–68.
Imamura, Y., et al., 2004. Azithromycin inhibits MUC5AC production induced by the Pseudomonas aeruginosa autoinducer *N*-(3-oxododecanoyl) homoserine lactone in NCI-H292 cells. Antimicrob. Agents Chemother. 48 (9), 3457–3461.
Inoue, Y., et al., 2014. ZIP2 protein, a zinc transporter, is associated with keratinocyte differentiation. J. Biol. Chem. 289 (31), 21451–21462.

Jackson, K.A., et al., 2008. Mechanisms of mammalian zinc-regulated gene expression. Biochem. Soc. Trans. 36 (6), 1262–1266.
Johannesson, B., et al., 2012. CFTR regulates early pathogenesis of chronic obstructive lung disease in βENaC-overexpressing mice. PLoS One 7 (8), e44059.
Kang, J.H., Hwang, S.M., Chung, I.Y., 2015. S100A8, S100A9 and S100A12 activate airway epithelial cells to produce MUC5AC via extracellular signal-regulated kinase and nuclear factor-κB pathways. Immunology 144 (1), 79–90.
Kaufman, R.J., 2002. Orchestrating the unfolded protein response in health and disease. J. Clin. Invest. 110 (10), 1389–1398.
Kim, J.H., et al., 2014. Regulation of the catabolic cascade in osteoarthritis by the zinc-ZIP8-MTF1 axis. Cell 156 (4), 730–743.
Kreda, S.M., Davis, C.W., Rose, M.C., 2012. CFTR, mucins, and mucus obstruction in cystic fibrosis. Cold Spring Harbor Perspectives Med. 2 (9), a009589.
Lang, C., et al., 2007. Anti-inflammatory effects of zinc and alterations in zinc transporter mRNA in mouse models of allergic inflammation. Am. J. Physiol. Lung Cell. Mol. Physiol. 292 (2), L577–L584.
Liang, X., Dempski, R.E., Burdette, S.C., 2016. Zn2+ at a cellular crossroads. Curr. Opin. Chem. Biol. 31, 120–125.
Liu, M.J., et al., 2013. ZIP8 regulates host defense through zinc-mediated inhibition of NF-κB. Cell Rep. 3 (2), 386–400.
Lu, W., 2004. Effects of dexamethasone on Muc5ac mucin production by primary airway goblet cells. Am. J. Physiol. Lung Cell. Mol. Physiol. 288 (1), L52–L60.
Luco, R.F., et al., 2011. Epigenetics in alternative pre-mRNA splicing. Cell 144 (1), 16–26.
Mall, M.A., Galietta, L.J.V., 2015. Targeting ion channels in cystic fibrosis. J. Cyst. Fibros. 14 (5), 561–570.
Mall, M., et al., 2004. Increased airway epithelial Na+ absorption produces cystic fibrosis-like lung disease in mice. Nat. Med. 10 (5), 487–493.
Miao, X., et al., 2013. Zinc homeostasis in the metabolic syndrome and diabetes. Front. Med. China 7 (1), 31–52.
Mizunoe, S., et al., 2012. Synergism between interleukin (IL)-17 and toll-like receptor 2 and 4 signals to induce IL-8 expression in cystic fibrosis airway epithelial cells. J. Pharmacol. Sci. 118 (4), 512–520.
Mocchegiani, E., et al., 1995. Role of the low zinc bioavailability on cellular immune effectiveness in cystic fibrosis. Clin. Immunol. Immunopathol. 75 (3), 214–224.
Nishimoto, Y., et al., 2010. Glycyrrhizin attenuates mucus production by inhibition of MUC5AC mRNA expression *in vivo* and *in vitro*. J. Pharmacol. Sci. 113 (1), 76–83.
Peters, J.L., et al., 2007. Targeting of the mouse Slc39a2 (Zip2) gene reveals highly cell-specific patterns of expression, and unique functions in zinc, iron, and calcium homeostasis. Genesis 45 (6), 339–352.
Prasad, A.S., 2013. Discovery of human zinc deficiency: its impact on human health and disease. Adv. Nutr. 4 (2), 176–190.
Prasad, A.S., et al., 2007. Zinc supplementation decreases incidence of infections in the elderly: effect of zinc on generation of cytokines and oxidative stress. Am. J. Clin. Nutr. 85 (3), 837–844.
Ron, D., Hubbard, S.R., 2008. How IRE1 reacts to ER stress. Cell 132 (1), 24–26.
Roscioli, E., et al., 2017. The uncoupling of autophagy and zinc homeostasis in airway epithelial cells as a fundamental contributor to COPD. Am. J. Physiol. Lung Cell. Mol. Physiol. 313 (17), L453–L465.
Sato, T., et al., 2012. STT3B-dependent posttranslational *N*-glycosylation as a surveillance system for secretory protein. Mol. Cell 47 (1), 99–110.
Shuto, T., et al., 2016. Pharmacological and genetic reappraisals of protease and oxidative stress pathways in a mouse model of obstructive lung diseases. Sci. Rep. 6, 39305.
Sugahara, T., et al., 2009. Calreticulin positively regulates the expression and function of epithelial sodium channel. Exp. Cell Res. 315 (19), 3294–3300.
Suico, M.A., et al., 2014. The transcription factor MEF/Elf4 is dually modulated by p53-MDM2 axis and MEF-MDM2 autoregulatory mechanism. J. Biol. Chem. 289 (38), 26143–26154.
Tamaki, M., et al., 2013. The diabetes-susceptible gene SLC30A8/ZnT8 regulates hepatic insulin clearance. J. Clin. Invest. 123 (10), 1–11.
Taylor, K.M., et al., 2012. Protein kinase CK2 triggers cytosolic zinc signaling pathways by phosphorylation of zinc channel ZIP7. Sci. Signal. 5 (210), ra11.
Ueno, K., et al., 2008. MUC1 mucin is a negative regulator of toll-like receptor signaling. Am. J. Respir. Cell Mol. Biol. 38 (3), 263–268.
Vallee, B.L., Falchuk, K.H., 1993. The biochemical basis of zinc physiology. Physiol. Rev. 73 (1), 79–118.
Van Biervliet, S., et al., 2007. Serum zinc concentrations in cystic fibrosis patients aged above 4 years: a cross-sectional evaluation. Biol. Trace Elem. Res. 119 (1), 19–26.
Van Biervliet, S., et al., 2008. The effect of zinc supplements in cystic fibrosis patients. Ann. Nutr. Metab. 52 (2), 152–156.
Wang, E.T., et al., 2008. Alternative isoform regulation in human tissue transcriptomes. Nature 456 (7221), 470–476.